Regulation by small RNAs via coupled degradation: Mean-field and variational approaches

Thierry Platini[*]

Virginia Bioinformatics Institute, Virginia Polytechnic Institute and State University, Blacksburg, Virginia 24061, USA

Tao Jia[†] and Rahul V. Kulkarni[‡]

Department of Physics, Virginia Polytechnic Institute and State University, Blacksburg, Virginia 24061, USA

Regulatory genes called small RNAs (sRNAs) are known to play critical roles in cellular responses to changing environments. For several sRNAs, regulation is effected by coupled stoichiometric degradation with messenger RNAs (mRNAs). The nonlinearity inherent in this regulatory scheme indicates that exact analytical solutions for the corresponding stochastic models are intractable. Here, we present a variational approach to analyze a well-studied stochastic model for regulation by sRNAs via coupled degradation. The proposed approach is efficient and provides accurate estimates of mean mRNA levels as well as higher-order terms. Results from the variational ansatz are in excellent agreement with data from stochastic simulations for a wide range of parameters, including regions of parameter space where mean-field approaches break down. The proposed approach can be applied for quantitative modeling of stochastic gene expression in complex regulatory networks.

PACS number(s): 82.39.Rt, 87.10.Mn, 87.17.Aa

I. INTRODUCTION

A new paradigm for cellular regulation has emerged in recent years with the discovery of novel noncoding genes called small RNAs (sRNAs). In bacteria, sRNAs often function as global regulators that mediate cellular adaptation to changing environments [1]. In higher organisms, the corresponding genes (microRNAs) are known to play key roles in the regulation of critical processes, such as development, stem cell pluripotency, and cancer [2,3]. It has been proposed that one of the key functions of sRNAs in controlling cellular processes is to regulate the variability (noise) in gene expression [3]. Recent experimental developments have led to approaches for quantifying such variability using single-molecule measurements of messenger mRNA (mRNA) levels [4]. These technological advances have now made possible experimental studies that analyze the roles of sRNAs in noise regulation during important cellular processes. Correspondingly, there is a need for theoretical approaches that complement such experimental efforts to enable a quantitative understanding of different mechanisms of sRNA-based regulation.

While the molecular mechanisms of sRNA-mediated regulation continue to be investigated, one established mechanism, representative of several bacterial sRNAs, corresponds to binding with mRNAs followed by coupled stoichiometric degradation [5]. An important challenge for current research is to analyze how this regulatory mechanism impacts the variability of gene expression across a population of cells. Several recent theoretical studies [6–12] have analyzed models based on the corresponding reaction scheme [shown in Fig. 1(a)]. The nonlinearity inherent in this reaction scheme implies that exact analytical solutions for the corresponding stochastic model are intractable; thus approximate analytical approaches are needed. Previous theoretical studies have primarily focused on

mean-field (MF) approaches and on steady-state distributions using expansions around MF solutions. However, MF approaches are not accurate when we have a combination of nonlinear reaction rates (due to an interaction with small RNAs) and low mRNA/sRNA levels, which point to the need for the development of alternative analytical approaches. Some recent approaches that go beyond the MF approximation involve methods for estimating the moments from the master equation [13,14]. It should further be noted that this model gives rise to a nonequilibrium stationary state for which the well-known detailed balance criterion is not valid. Therefore, as with many biological processes, this model is representative of the broader class of nonequilibrium processes for which it is desirable to develop analytical approaches that go beyond MF approaches.

In this paper, we analyze stochastic models of sRNA-based regulation via coupled degradation [as shown in Fig. 1(a)] . We first discuss the MF approximation, which corresponds to neglecting mRNA-sRNA correlations, and define dimensionless variables that are useful in quantifying deviations between MF results and data from stochastic simulations. To go beyond MF, we use a variational approach which has been successfully applied to gene regulatory networks in recent work [15–18]. Within this approach, we present a general ansatz for the steady-state probability distribution which, at the simplest level, reduces to the MF approximation. At the next level, the variational ansatz gives results that are in excellent agreement with data from simulations for the mean and variance of the regulated mRNA distribution.

II. MASTER EQUATION AND MEAN-FIELD APPROACH

We begin by considering the kinetic scheme presented in Fig. 1(a). The probability distribution of mRNA and sRNA levels per cell, $P_{m,s}(t)$, obeys the master equation

$$
\begin{aligned}
\partial_t P_{m,s} = {} & k_m P_{m-1,s} + k_s P_{m,s-1} + \mu_m(m+1) P_{m+1,s} \\
& + \mu_s(s+1) P_{m,s+1} + \gamma(m+1)(s+1) P_{m+1,s+1} \\
& - (k_m + k_s + \mu_m m + \mu_s s + \gamma ms) P_{m,s},
\end{aligned} \tag{1}
$$

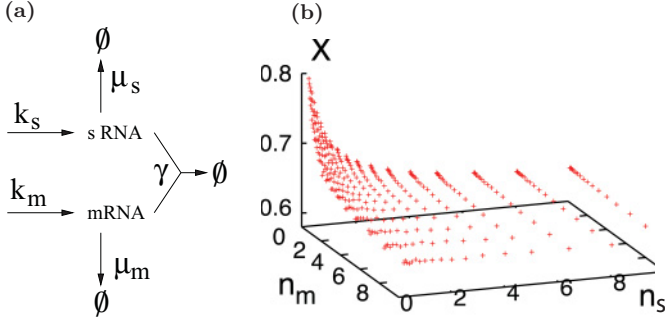[*]platini@vbi.vt.edu
[†]tjia@vt.edu
[‡]kulkarni@vt.edu

FIG. 1. (Color online) (a) Kinetic scheme for regulation of mRNA by small RNAs with coupled degradation rate γ. (b) Ratio $X = \langle m \rangle / n_m$, obtained from simulation data, is plotted as a function of n_m and n_s. Parameters are chosen such that $\epsilon_m = \epsilon_s = 1$ and $\gamma = 1$. For $n_m, n_s \gg 1$, X converges toward the MF prediction ($X \simeq 0.618$).

where k_j, μ_j ($j = m, s$), and γ are the parameters defined in Fig. 1(a). We will focus on the stationary distribution, denoted by $P_{m,s}^*$. It is convenient to define the following set of independent dimensionless parameters

$$\epsilon_m = \frac{k_s \gamma}{\mu_m \mu_s}, \quad \epsilon_s = \frac{k_m \gamma}{\mu_m \mu_s}, \quad n_m = \frac{k_m}{\mu_m}, \quad n_s = \frac{k_s}{\mu_s}. \quad (2)$$

From the master equation (1), we derive the following exact equations

$$\partial_t \langle m \rangle = k_m - \mu_m \langle m \rangle - \gamma \langle ms \rangle, \quad (3)$$

$$\partial_t \langle s \rangle = k_s - \mu_s \langle s \rangle - \gamma \langle ms \rangle. \quad (4)$$

In the stationary state, we can explicitly relate the average mRNA and sRNA levels to the correlation term $\langle ms \rangle^*$ [19,20] via

$$\frac{1}{\epsilon_m} \left(1 - \frac{\langle m \rangle^*}{n_m} \right) = \frac{1}{\epsilon_s} \left(1 - \frac{\langle s \rangle^*}{n_s} \right) = \frac{\langle ms \rangle^*}{n_m n_s}, \quad (5)$$

where $\langle \ldots \rangle^*$ denotes the stationary average. More generally, moments at one level are coupled to higher-order moments due to the nonlinear interaction term. This hierarchy makes the exact solution of the master equation intractable. Defining

$$X = \frac{\langle m \rangle^*}{n_m}, \quad Y = \frac{\langle s \rangle^*}{n_s}, \quad \text{and} \quad C = \frac{\langle ms \rangle^*}{\langle m \rangle^* \langle s \rangle^*}, \quad (6)$$

Eq. (5) leads to

$$\frac{1 - X}{\epsilon_m} = \frac{1 - Y}{\epsilon_s} = CXY. \quad (7)$$

The traditional MF approximation consists of neglecting correlations through the substitution $\langle ms \rangle^* \rightarrow \langle m \rangle^* \langle s \rangle^*$. This assumption thus corresponds to $C = 1$ and leads to

$$\epsilon_m XY + X - 1 = 0, \quad \epsilon_s XY + Y - 1 = 0. \quad (8)$$

Comparing Eqs. (5) and (7), we see that the *exact* means [i.e., solutions of Eq. (5)] are generated by the MF solutions considered with the rescaled interaction parameter $\gamma' = C\gamma$. Determination of C can therefore provide accurate estimates of the mean mRNA and sRNA levels. The ratio C is also an indicator of the accuracy of MF results: the MF is a good approximation when $C \simeq 1$, whereas deviations from unity

indicate that better approximations are needed. Furthermore, note that X and Y are, in general, functions of the four parameters ϵ_m, ϵ_s, n_m, and n_s; however the MF approximation (7) predicts that both quantities depend only on ϵ_m and ϵ_s. It follows that MF theory breaks down in regions of parameter space where X and Y depend on the parameters n_m and n_s (for fixed ϵ_m and ϵ_s). These regions are indicated by significant deviations between the exact ratio X (Y) and the solution λ_+ (λ_-) of Eq. (8).

We now analyze deviations of the MF results from stochastic simulations data obtained using the Gillespie algorithm [21]. The ratios X and C are plotted in Figs. 1(b) and 2(a) respectively. These data are presented as a function of n_m and n_s, keeping ϵ_m and ϵ_s constant. The figures indicate that both quantities converge toward the MF predictions in the limit $n_s, n_m \gg 1$ ($X \rightarrow 0.618$ and $C \rightarrow 1$). From Eq. (7), it can be seen that deviations of the exact value of X from the mean-field predictions are driven by the deviations of C from the MF predictions. We see that as $C \rightarrow 1$ one has $X \rightarrow \lambda_+$, i.e., the mean-field prediction becomes exact. In other words, C and X behave the same way. More significantly, the data shows that MF is not a good approximation for small n_m and n_s. This is important to note since, in several cellular systems, mRNA abundances can be low (i.e., n_m is small) [22]. This indicates that more accurate approximations are needed in such cases.

Furthermore, in the uncorrelated approximation, the stationary probability distribution can be written as the product of Poisson distributions

$$P_{m,s}^* \approx \Pi_{\lambda_+}(m) \times \Pi_{\lambda_-}(s), \quad (9)$$

where $\Pi_x(n) = e^{-x} x^n / n!$. Defining the marginal distributions $P_m^* = \sum_s P_{m,s}^*$ and $P_s^* = \sum_m P_{m,s}^*$, the ratios

$$d_m = \frac{\langle m \rangle^*}{\langle m^2 \rangle^* - (\langle m \rangle^*)^2}, \quad d_s = \frac{\langle s \rangle}{\langle s^2 \rangle^* - (\langle s \rangle^*)^2} \quad (10)$$

measure deviations between the marginals (P_j^*, $j = m, s$) and the simple Poisson distribution. Again, deviations of $D = d_s d_m$ from unity reveal that both marginal probability distributions cannot be approximated by the Poisson distribution. In Fig. 2(b), stochastic simulations data indicate that D deviates significantly from 1 for large n_m and n_s. This observation implies that higher-order terms, such as $\langle m^2 \rangle$ and $\langle s^2 \rangle$, cannot be obtained using the MF prediction $\langle j^2 \rangle - \langle j \rangle^2 = \langle j \rangle$ ($j = m, s$), even in regions of parameter space for which the mean values are given accurately by the MF approximation. From the master equation, in the stationary state, one can derive the following exact equation

$$\langle m^2 \rangle^* = \frac{k_m}{\mu_m} (\langle m \rangle^* + 1) - \frac{\gamma}{\mu_m} \langle m^2 s \rangle^*, \quad (11)$$

which indicates that it is only in regions of parameter space where $\langle m^2 s \rangle^* \simeq \langle m^2 \rangle^* \langle s \rangle^*$ that the uncorrelated (MF) approximation can give an accurate estimate of the variance (even assuming that the MF result for the mean is accurate). In regions of parameter space such that X and C match the MF solution, the condition $\langle m^2 s \rangle \simeq \langle m^2 \rangle \langle s \rangle$ is not necessarily a good approximation, hence the discrepancy for D. Interestingly, it is for small parameter values n_j ($j = m, s$), for which the MF approximation does not give accurate values, that D
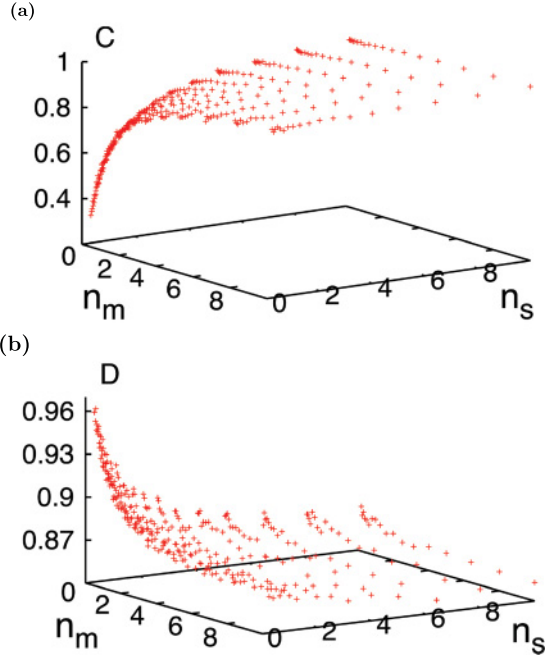
FIG. 2. (Color online) Stationary value of (a) $C = \langle ms \rangle / \langle m \rangle \langle s \rangle$ and (b) $D = d_m d_s$, obtained from simulation data, plotted as a function of n_m and n_s. We keep $\epsilon_m = \epsilon_s = 1$ and $\gamma = 1$.

approaches 1. This indicates that the Poisson distribution is in some way embedded in the structure of $P_{m,s}^*$.

III. VARIATIONAL APPROACH

A. Method

Based on the preceding analysis, it seems natural to approximate $P_{m,s}^*$ as a superposition of Poisson distributions. This approximation can be implemented using the variational method introduced by Eyink [23], combined with the quantum Hamiltonian formalism of the master equation [15,16]. Following the mapping outlined by Doi [24], we first define the state vector $|m,s\rangle$ of m and s mRNA and sRNA macromolecules, respectively. Following the mapping outlined by Doi [24], the operators $a^\dagger$ (a) and $b^\dagger$ (b) associated with the creation (annihilation) of mRNA and sRNA respectively, are introduced:

$$a^\dagger |m,s\rangle = |m+1,s\rangle, \tag{12}$$

$$b^\dagger |m,s\rangle = |m,s+1\rangle, \tag{13}$$

$$a|m+1,s\rangle = (m+1)|m,s\rangle, \tag{14}$$

$$b|m,s+1\rangle = (s+1)|m,s\rangle. \tag{15}$$

They obey the commutation relation $[a,a^\dagger] = [b,b^\dagger] = 1$. From the normalized vacuum state $|0,0\rangle$, any state $|m,s\rangle$ is generated via

$$|m,s\rangle = (a^\dagger)^m (b^\dagger)^s |0,0\rangle, \tag{16}$$

with $\langle m,s|m',s'\rangle = \delta_{m,m'} \delta_{s,s'} m! s!$. Let us now define $|\psi\rangle(t)$ by

$$|\psi\rangle(t) = \sum_{m,s} P_{m,s}(t) |m,s\rangle, \tag{17}$$

and rewrite the master equation (1) under the compact form $\partial_t |\psi(t)\rangle = -\mathcal{L}|\psi(t)\rangle$ with

$$\mathcal{L} = k_m + k_s + \mu_m a^\dagger a + \mu_s b^\dagger b + \gamma a^\dagger a b^\dagger b$$
$$- (k_m a^\dagger + k_s b^\dagger + \mu_m a + \mu_s b + \gamma ab). \tag{18}$$

Focusing on the stationary state, we denote by $\langle \psi_L|$ and $|\psi_R\rangle$ the left and right eigenstates with vanishing eigenvalue. They obey $\langle \psi_L|n,m\rangle = \langle \psi_L|\psi_R\rangle = 1$. The mapping to the original problem is given by

$$P_{m,s}^* = \frac{\langle m,s|\psi_R \rangle}{m! s!}. \tag{19}$$

To initiate the variational ansatz, we define the left and right trial vectors ($\langle \phi_L(\Lambda_L)|$ and $|\phi_R(\Lambda_R)\rangle$), constructed using a set of independent parameters, Λ_L and Λ_R. Defining the functional $\mathcal{H}(\Lambda_L, \Lambda_R) = \langle \phi_L|\mathcal{L}|\phi_R \rangle$, the eigenstates are determined using the variational principle $\delta \mathcal{H} = 0$. A detailed explanation of the variational scheme is provided in [23].

We now generalize the uncorrelated approximation to propose a specific ansatz for the trial vectors as the superposition of Poisson distributions. A similar ansatz has also been proposed in a recent study of reaction systems including different chemical species [18]. We define

$$\langle \phi_L(\Lambda_L)| = \langle 0,0|e^{a+b} \prod_{i,j=0}^{d} e^{\theta_{i,j} a^i b^j}, \tag{20}$$

$$|\phi_R(\Lambda_R)\rangle = \sum_{i,j=1}^{d} \Theta_{i,j} e^{\alpha_i(a^\dagger - 1)} e^{\beta_j(b^\dagger - 1)} |0,0\rangle, \tag{21}$$

with $\Lambda_R = \{\alpha_p, \beta_q, \Theta_{p,q}\}$ and $\Lambda_L = \{\theta_{p,q}\}$ ($\theta_{d,d} = 0$). In each vector, the total number of parameters $\mathcal{N}$ is given by $\mathcal{N} = d(d+2)$. The parameters of $\langle \phi_L|$ are imposed by the condition $\langle \phi_L|m,n\rangle = 1$ which leads to $\theta_{p,q} = 0, \forall p, q$. It follows that the set Λ_R is the solution of $\langle \delta \phi_L|\mathcal{L}|\phi_R\rangle|_{\Lambda_L = \{0\}} = 0$. In other words, Λ_R is the solution of the set of equations generated by $\partial_{\theta_{i,j}} \langle \phi_L|\mathcal{L}|\phi_R\rangle|_{\Lambda_L = \{0\}} = 0$ for $i,j = 0,1,2,\ldots,d$ with the pair $(i = d, j = d)$ excluded. Using the relation

$$\partial_{\theta_{i,j}} \langle \phi_L|_{\Lambda_L = \{0\}} = \langle 0,0|e^{a+b} a^i b^j = \sum_{m,s} \frac{\langle m+i,s+j|}{m! s!}, \tag{22}$$

our calculation leads to the system of equations

$$\sum_{p,q=1}^{d} \Theta_{p,q} \alpha_p^i \beta_q^j \times [\epsilon_s \epsilon_m (ij + i\beta_q + j\alpha_p)$$
$$+ i n_s \epsilon_s (1 - n_m/\alpha_p) + j n_m \epsilon_m (1 - n_s/\beta_q)] = 0, \tag{23}$$

generated for $i,j = 0,1,2,\ldots,d$ with the pair $(i = d, j = d)$ excluded. The first equation (for $i = j = 0$), corresponds to the probabilistic interpretation $\langle \phi_L|\phi_R\rangle = 1$ and leads to the normalization constraint $\sum_{p,q} \Theta_{p,q} = 1$. From Eq. (23) one can then generate the $\mathcal{N}$ independent conditions required to determine the right eigenvector parameters. It follows

that an approximation of the stationary distribution is given by

$$\mathcal{P}_{m,s}^* = \frac{\langle m,s|\phi_R(\Lambda_R^*)\rangle}{m!s!}, \tag{24}$$

where $\Lambda_R^* = \{\alpha_p^*, \beta_q^*, \Theta_{p,q}^*\}$ is the solution of Eq. (23). The latter distribution can be explicitly written as a superposition of Poisson distributions

$$\mathcal{P}_{m,s}^* = \sum_{p,q} \Theta_{p,q}^* \Pi_{\alpha_p^*}(m) \Pi_{\beta_q^*}(s). \tag{25}$$

We note that the MF results are recovered by considering the ansatz with $d = 1$. In this case, $\mathcal{P}_{m,s}^*$ is simply a product of two Poisson distributions with means α and β, respectively. The variational equations give $n_s(n_m - \alpha) - \epsilon_m \alpha \beta = 0$ and $n_m(n_s - \beta) - \epsilon_m \alpha \beta = 0$, leading to $C = D = 1$.

B. Comparison with stochastic simulations

Going one step beyond the MF approximation, we consider the ansatz (21) with $d = 2$. We first consider the symmetric case $k_m = k_s = k$ and $\mu_m = \mu_s = \mu$. This choice imposes $\alpha_j = \beta_j$ ($j = 1,2$) and $\Theta_{1,2} = \Theta_{2,1}$. The set Λ_R^*, the solution of the equations generated by Eq. (23), is obtained numerically using standard routines. From a practical point of view, the numerical calculation is significantly faster than stochastic simulations, especially if we need to explore large regions of parameter space.

Figure 3(a) presents a comparison of our results with data from stochastic simulations. Keeping the ratios ϵ_m and ϵ_s constant, the quantities X, C, and D are plotted as a function of μ for $\gamma = 1$, 5, and 10. Clearly, deviations from MF results appear more pronounced as γ increases. However, for a range of parameter values μ and even for a large mRNA-sRNA coupling, the variational scheme gives accurate values of the mean mRNA level per cell ($\langle m \rangle^* = X n_m$). Additionally, we checked that the predictions for $\langle s \rangle^*$ also present an excellent agreement with simulation data. Importantly, the agreement of our predictions with simulation data, for the quantities C and D, shows that the variational method also gives accurate values of higher-order terms, such as the correlation $\langle ms \rangle^*$ ($= C \langle m \rangle^* \langle s \rangle^*$) and variance $\langle j^2 \rangle^* - (\langle j \rangle^2)^*$ ($= \langle j \rangle^*/d_j$).

To compare our results in the nonsymmetric case, we consider variations in μ_m, keeping $\mu_s = 2$ and $\gamma = 1$ fixed. The set of parameters is computed numerically, solving *eight* coupled equations generated from Eq. (23). The ratio ϵ_s is kept equal to unity while $\epsilon_m = 4$, 1, and 1/4. As shown in Fig. 3(b), the ansatz predictions are, once again, in excellent agreement with simulation data.

IV. CONCLUSION

The variational approach presented can be generalized to more complex networks and nonequlilibrium steady states involving multiple interacting species. As in the current work, the initial step is to obtain the marginal distributions for the different interacting species using a MF approximation. Since mean field effectively reduces the problem to one of noninteracting species in effective fields, it should, in general, be straightforward to obtain these marginal distributions. The Ansatz proposed involves weighted combinations of the
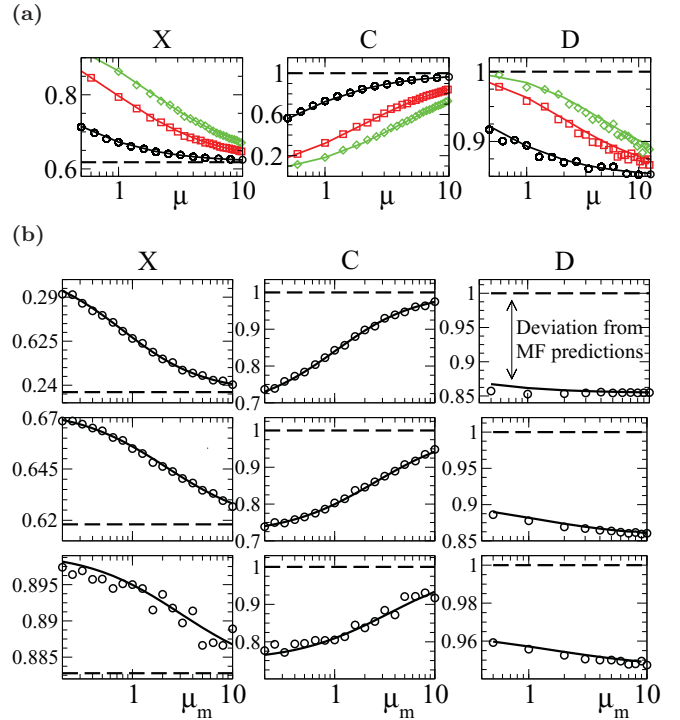

FIG. 3. (Color online) Comparisons of the quantities $X = \langle m \rangle / n_m$, $C = \langle ms \rangle / \langle m \rangle \langle s \rangle$, and $D = d_s d_m$ extracted from simulation data (symbols) with the ansatz predictions (lines) and MF results (dashed lines). (a) Data are plotted as a function of $\mu = \mu_m = \mu_s$ on a logarithmic scale for $\gamma = 1$ (black circles), $\gamma = 5$ (red squares), and $\gamma = 10$ (green diamonds). We keep $\epsilon_m = \epsilon_s = 1$ with $k_m = k_s = k$. (b) Data are plotted as a function of μ_m on a logarithmic scale for $\epsilon_m = 4$ (top), $\epsilon_m = 1$ (middle), and $\epsilon_m = 1/4$ (bottom). We keep $\mu_s = 2$, $\gamma = 1$, and $\epsilon_s = 1$.

products of these marginal distributions, where the weight of each term and the scale parameters of each marginal are the variational parameters. These parameters are obtained by solving the set of coupled equations generated with the variational method. At the lowest order, the approach will recover the MF results for the mean values, whereas going to higher orders will yield systematic improvements over the MF results and accurate estimates for the higher moments. In particular, at second order, the approach results in a simple set of algebraic equations which can be solved to get accurate estimates of the means and variances for the interacting species. The results derived will aid approaches for inference of model parameters from experimental measurements of mean and variance. It is hoped that future work coupling such approaches with experiments will lead to the quantitative understanding of gene expression in complex networks.

[1] S. Gottesman, Trends Genet. **21**, 399 (2005).

[2] M. Inui, G. Martello, and S. Piccolo, Nat. Rev. Mol. Cell Biol. **11**, 252 (2010).

[3] E. Hornstein and N. Shomron, Nat. Genet. **38**, S20 (2006).

[4] A. Raj and A. van Oudenaarden, Ann. Rev. Biophys. **38**, 255 (2009).

[5] E. Masse, F. Escorcia, and S. Gottesman, Genes Dev. **17**, 2374 (2003).

[6] E. Levine and T. Hwa, Curr. Opin. Microbiol. **11**, 574 (2008).

[7] E. Levine, Z. Zhang, T. Kuhlman, and T. Hwa, PLoS Biol. **5**, e229 (2007).

[8] N. Mitarai, A. M. Andersson, S. Krishna, S. Semsey, and K. Sneppen, Phys. Biol. **4**, 164 (2007).

[9] P. Mehta, S. Goyal, and N. S. Wingreen, Mol. Syst. Biol. **4**, 221 (2008).

[10] V. P. Zhdanov, Biosystems **95**, 75 (2009).

[11] Y. Jia, W. Liu, A. Li, L. Yang, and X. Zhan, Biophys. Chem. **143**, 60 (2009).

[12] Y. Shimoni, G. Friedlander, G. Hetzroni, G. Niv, S. Altuvia, O. Biham, and H. Margalit, Mol. Syst. Biol. **3**, 138 (2007).

[13] B. Barzel and O. Biham, Astrophys. J. **658**, L37 (2007).

[14] B. Barzel and O. Biham, Phys. Rev. Lett **106**, 150602 (2011).

[15] M. Sasai and P. G. Wolynes, Proc. Natl. Acad. Sci. USA **100**, 2374 (2003).

[16] Y. Lan, P. G. Wolynes, and G. A. Papoian, J. Chem. Phys. **125**, 124106 (2006).

[17] J. Ohkubo, J. Stat. Mech. (2007) P09017.

[18] J. Ohkubo, J. Chem. Phys. **129**, 044108 (2008).

[19] V. Elgart, T. Jia, and R. V. Kulkarni, Biophys. J. **98**, 2780 (2010).

[20] E. Levine, M. Huang, Y. M. Huang, T. Kuhlman, H. Shi, Z. Zhang, and T. Hwa J. Chem. Phys. **129**, 1-8 (2008).

[21] D. T. Gillespie, J. Phys. Chem. **81**, 2340 (1977).

[22] S. Kar, W. T. Baumann, M. R. Paul, and J. J. Tyson, Proc. Natl. Acad. Sci. USA **106**, 6471 (2009).

[23] G. L. Eyink, Phys. Rev. E **54**, 3419 (1996).

[24] M. Doi, J. Phys. A **9**, 1465 (1976).